General Disclaimer

One or more of the Following Statements may affect this Document

- This document has been reproduced from the best copy furnished by the organizational source. It is being released in the interest of making available as much information as possible.

- This document may contain data, which exceeds the sheet parameters. It was furnished in this condition by the organizational source and is the best copy available.

- This document may contain tone-on-tone or color graphs, charts and/or pictures, which have been reproduced in black and white.

- This document is paginated as submitted by the original source.

- Portions of this document are not fully legible due to the historical nature of some of the material. However, it is the best reproduction available from the original submission.

Produced by the NASA Center for Aerospace Information (CASI)

THIN FILM ATOMIC HYDROGEN DETECTORS

FINAL REPORT

CONTRACT NAS 5-23470

Prepared for

NATIONAL AERONAUTICS AND SPACE ADMINISTRATION

GODDARD SPACE FLIGHT CENTER

GREENBELT, MD.

submitted by

Dr. C. L. Gruber

Electrical Engineering Department

SOUTH DAKOTA SCHOOL OF MINES AND TECHNOLOGY

RAPID CITY, SOUTH DAKOTA

June 1977

ABSTRACT

Thin film and bead thermistor atomic surface recombination hydrogen detectors were investigated both experimentally and theoretically. Devices were constructed on a thin Mylar film substrate. Using suitable Wheatstone bridge techniques sensitivities of 80 $\mu V/2 \cdot 10^{13}$ atoms/sec are attainable with response time constants on the order of 5 seconds.

TABLE OF CONTENTS

LIST OF FIGURES

I. INTRODUCTION

Measurement of atomic hydrogen beam flux in hydrogen maser atomic clock systems has proven to be a very significant problem throughout their period of development. RF dissociators used for atomic beam generation are subject to marked fluctuations in output beam intensity on both long and short time scales. Fluctuations in intensity can appreciably affect performance of the clock system especially if the flux drops below threshold, even on a transient basis. Atomic beam clocks in addition require a relatively fast high sensitivity atom detector for any mode of operation. Evaluation and improvement of existing dissociator systems requires a means of quantitatively measuring the atomic production efficiency and projected service lieftimes. It is toward the latter end this project is directed.

Over the previous decade or more numerous physical mechanisms have been investigated for application to atomic beam detection and measurement.[1] Only three such mechanisms have shown any real promise for application to a practical device;

1. Thermal detection of atomic surface recombination energy (4.4 ev/event for hydrogen on suitable metallic surfaces).

2. Electron beam bombardment with selective ionization or resonance excitation of hydrogen beam atoms.

3. Optical radiation resonance absorption in the discharge dissocatior bulb.

Other mechanisms may exhibit some potential but have not been explored as yet.

Previous work on a metal (platinum) bolometer[2] thermal detector has indicated excellent potential for such a device. In this investigation we

attempt to expand upon this principle in obtaining increased sensitivity, better structural strength and stability and improved noise characteristics. As with all thermal detectors slow response time accompanies high sensitivity in addition to sensitivity to the thermal ambient conditions.

II. DEVICE MODELS

A. PHYSICAL MODEL

Thermal energy flux detectors, depending upon the release of (atomic recombination) energy to a suitable solid surface, require the measurement of a bulk material temperature to obtain a value for the energy flux. The temperature of the surface depends not only upon the incident beam energy flux but also on the various heat loss mechanisms at the material surface such as bulk thermal conduction and black-body radiation to and from the surrounding environment. Ultimate equilibrium surface temperature is determined by the balance of heat gain and loss from the detector surface.

For the purposes of thermal analysis of a typical detector structure, figure 1 is assumed to be a representative physical structure. A rectangular geometry is chosen for convenience only since circular cylindrical detector elements have been often used. In any case the following analysis is applicable.

We assume a supporting substrate of length D, width W, and thickness t, composed of material with thermal conductivity $K_s \frac{W \cdot M}{M^2 \cdot ^0C}$, specific heat $C_s - \frac{J}{Kg \cdot ^0C}$, and density $P_s - \frac{Kg}{m^3}$. The substrate is thermally and mechanically bonded at either end to (assumed) infinite heat sinks at temperature T_H.

The atomic recombination or active surface of suitably chosen material (Platinum in our case) is assumed to be negligibly thin with respect to the substrate dimension t and to cover a region of length L centered on the substrate, and extending across the full width W as shown. We assume the surface material has neglible mass hence non-radiative heat transfer properties are determined by the substrate alone. To meet this condition,

$$\frac{t_f}{t} < \frac{K_s}{K_f}$$

where t_f is the surface film thickness and K_f is its thermal conductivity.

SURROUNDINGS AT TEMPERATURE T_O

F — INCIDENT ATOMIC BEAM FLUX

ACTIVE RECOMBINATION SURFACE AT TEMPERATURE T_l

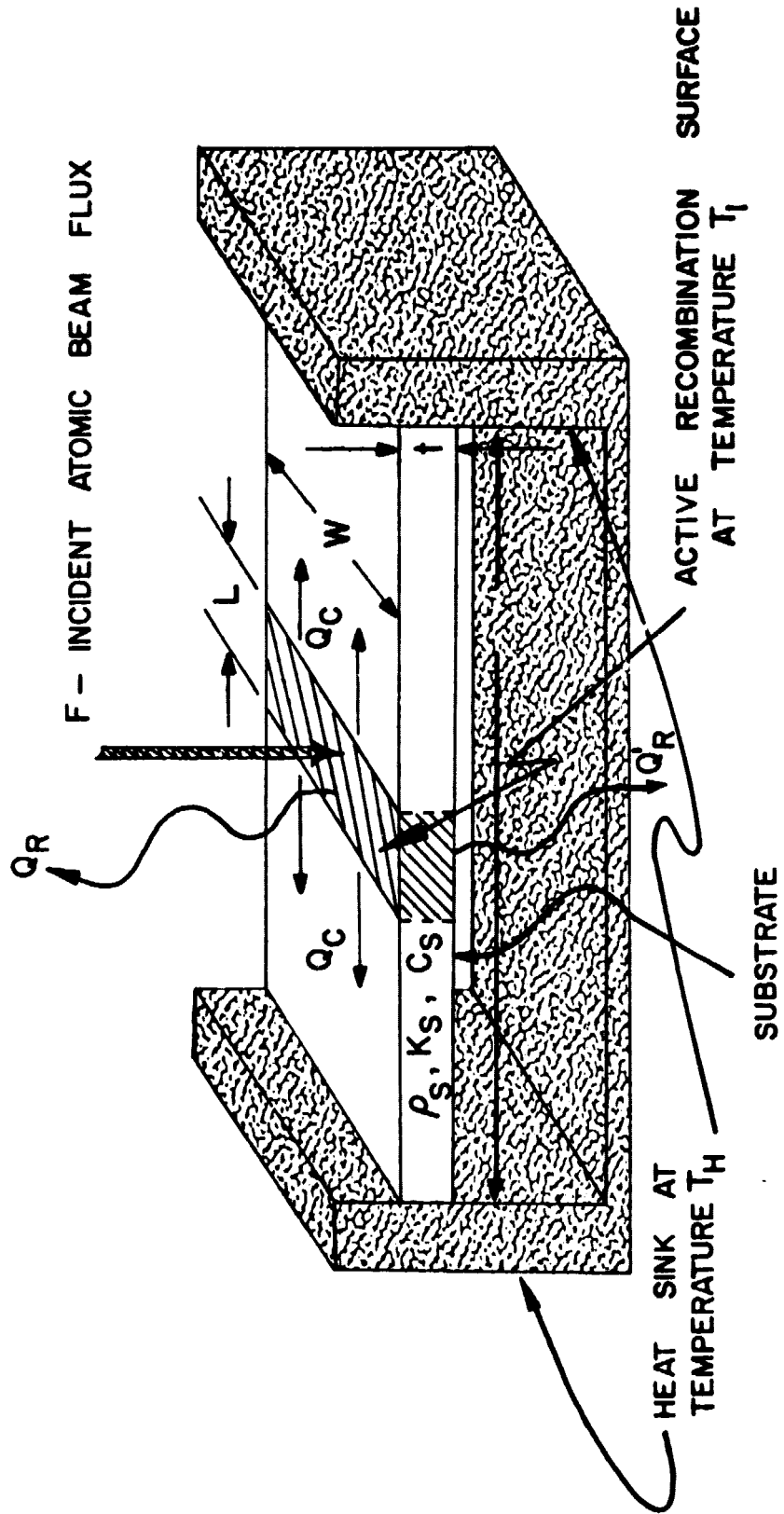SUBSTRATE

HEAT SINK AT TEMPERATURE T_H

FIGURE 1

PHYSICAL STRUCTURE

Most of the present analysis will further assume that the substrate is sufficiently thin to justify certain one-dimensional heat flow assumptions especially for heat conduction parallel to the substrate surface. For the heat fluxes considered here this assumption is also well justified for flow perpendicular to the surface since as will be shown later,

$$\frac{Q_B \, t}{K_s} \ggg \Delta T$$

where Q_B is the atomic recombination energy flux and ΔT is the temperature differential between top and bottom surfaces of the film.

B. THERMAL MODEL

For the purposes of thermal modelling a detector element, a simpler structure than that of figure 1 is used as shown in figure 2. Several independent heat
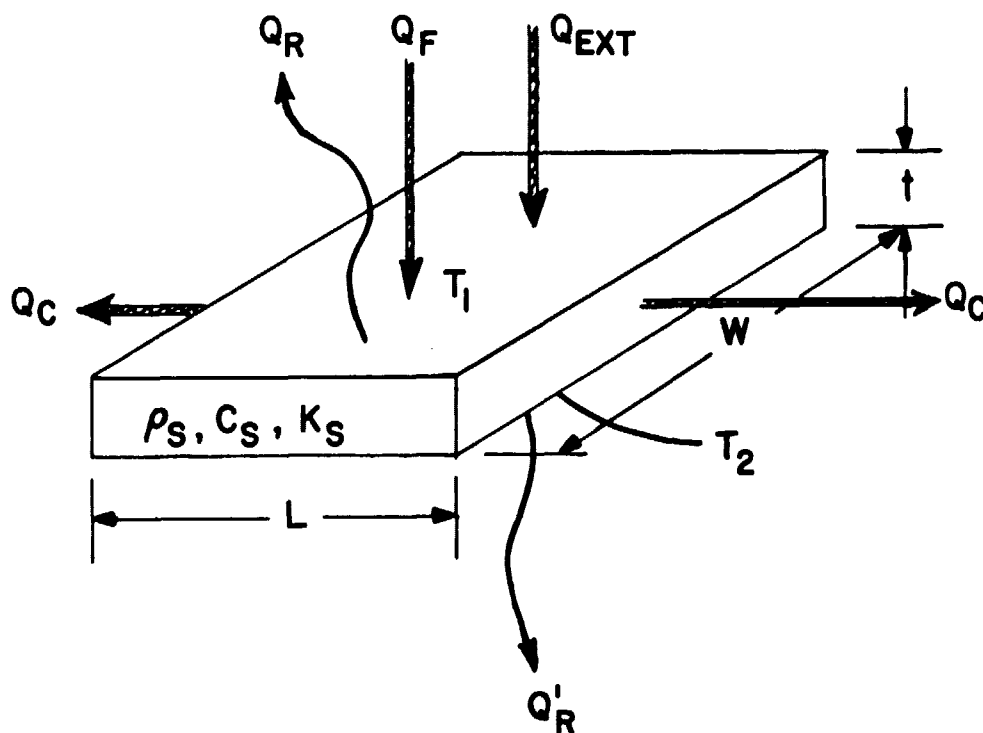

FIGURE 2

THERMAL MODEL

energy fluxes are considered significant in the model: $Q_f = FE\eta$, the atomic beam energy flux in watts/m^2, with F the incident atomic beam particle flux, $\frac{atoms}{m^2}$, E the recombination energy, 4.4 ev, and η the surface recombination efficiency ($\eta < .5$); Q_c, the conductive heat transfer rate in the substrate as shown on fig. 1; Q_R the net radiative heat transfer rate between the recombination surface and the surroundings, at temperature T_o, Q'_R the net radiative heat transfer rate between the substrate and the surrounding heat sink (assumed to be continuous beneath the substrate) at temperature T_H; Q_{ext} represents any external source (not shown) of heat supplied uniformly to either the top or bottom surfaces of the substrate by ohmic heating for instance. Figure 2 shows the region of the substrate hereafter called the active region encompassing the recombination surface and the substrate beneath it. Energy fluxes are as shown.

B.1. THERMAL EQUILIBRIUM

At thermal equilibrium of course the net energy flux from the active region must be zero at the prevailing equilibrium temperatures, T_1 on the top surface, T_2 on the bottom, hence,

$$Q_R + Q'_R + 2Q_c \frac{t}{L} = Q_f + Q_{ext} = Q_T \tag{1}$$

The radiative heat transfer terms can be linearized for small temperature differences ($\Delta T \leq 15^o C$) and referenced to the surrounding temperature level appropriate to the surface in question, T_o for the top of the substrate, T_H for the bottom. We will assume an emissivity for the recombination (top) surface $\varepsilon < 1$ and for the presumed to be uncoated lower substrate surface $\varepsilon = 1$. The radiative terms under these conditions become approximately

$$Q_R = 4\sigma T_o^3 \varepsilon (T_1 - T_o) \quad watt/m^2$$

$$Q'_R = 4\sigma T_H^3 (T_2 - T_H) \quad watt/m^2 \tag{2}$$

$$\sigma = 5.76 \times 10^{-8} \quad watts/m^2 \cdot {}^o K^4$$

For a first approximation to the basic heat flow model we will assume that $Q_c \frac{t}{L}$ can be neglected compared with the radiation terms and that a linear temperature gradient across the substrate exists (one-dimensional heat flow). Under these conditions detailed heat flow balancing applied to the top and bottom surfaces gives,

$$Q - Q_R = K_s \frac{T_1 - T_2}{t} = Q'_R - Q' \tag{3}$$

where Q, Q' are external heat fluxes introduced at the top and bottom surfaces of the substrate respectively.

Solving for the temperature difference between top and bottom surfaces, $T_2 - T_1$, and absolute temperature of the bottom surface (facing the holder) we get,

$$T_1 - T_2 \cong \frac{\sigma\epsilon (T_o^4 - T_H^4) + (Q - \epsilon Q')}{(1 + \epsilon) K_s/t} \tag{4}$$

$$T_2^4 \cong \frac{1}{1+\epsilon} \left(T_H^4 + \epsilon T_o^4 \right) + \frac{1}{\sigma} (Q + Q') \tag{5}$$

From Eq. 4 we can infer that conductive heat flow through the substrate thickness is sufficiently great as to render opposite surfaces at essentially the same temperature if $t < 0.1$ mm.

If we consider the effect of heat conduction <u>parallel</u> to the substrate surface, Q_c, the heat balance must include the difference in heat flow areas parallel and perpendicular to the substrate surface as well as the coupling between surface radiative heat transfer and conductive heat flow away from the active region.

To determine the temperature profile parallel to the substrate, we define, z, as the distance from the edge of the (assumed isothermal) active region at

temperature T_2 toward the junction between holder and substrate. T_∞ is the mean substrate equilibrium temperature at large distance from the active region, established by radiative heat transfer between the substrate and the surroundings, $T_\infty^4 = (\dfrac{T_H^4 + T_o^4}{2})$. The differential equation for $\Delta T(z) = T(z) - T_\infty$ is

$$K_s t \frac{d^2 \Delta T(z)}{dy^2} = 8\sigma T_x^3 \Delta T(z)$$

where $\qquad T_x^3 = \left\langle \frac{(T^2(z) + T\infty^2)(T(z) + T_\infty)}{4} \right\rangle$

Assuming T_x^3 is approximately constant with $T(z) = T_2$, the solution to the differential equation is,

$$\Delta T(z) = \Delta T_o e^{-\alpha z} \tag{6}$$

where $\Delta T_o = T_2 - T_\infty$

and $\qquad \alpha = \sqrt{\dfrac{8 \sigma T_x^3}{K_s t}} \tag{6a}$

$1/\alpha = L_D$ is an effective "diffusion length" for heat flow parallel to the surface of the substrate. At the edge of the active region,

$$Q_c = -K_s \frac{d\Delta T(z)}{dz}\bigg|z = 0$$

$$= \frac{K_s \Delta T_o}{L_D} \quad \text{watts/m}^2 \tag{7}$$

is the conductive heat loss rate from the active region.

L_D can be further physically interpreted in terms of the approximate radius of the "circle of influence" of a point heat source applied to the substrate surface. At a distance of approximately $3L_D$ the temperature perturbation resulting

from such a point source is negligible compared with that at the point of application (reduced by a factor greater than 20).

Based upon the above argument, any thermal detector system structurally similar to the one shown in figure 1 should be designed with the length of the surface active region

$$L > 2L_D$$

for optimum radiation limited, temperature sensitivity. Moreover to avoid additional heat loss to the holder by conduction through the ends of the substrate, the edge of the active region should be separated from the holder by a distance,

$$x = \frac{D - L - 6L_D}{2} \tag{8}$$

The above expressions represent the basic design equations for the thin substrate thermal sensor. One final consideration must be examined, namely the neglecting of heat flow, Q_c, with respect to the radiative heat transfer rates. This ratio is

$$\frac{2 Q_c}{Q_R + Q'_R} = \frac{2}{4} \frac{K_s (T_2 - T_\infty) Wt}{\sigma T_x^3 (T_2 - T_H) WL} \frac{8 \sigma T_x^3}{K_s t} \frac{1}{1 + \epsilon}$$

$$\approx 2 \sqrt{2} \frac{L_D}{L} \tag{9}$$

which is small if the design conditions are met. Alternatively we can compare $2Q_c$ with heat conduction through the film thickness, however the latter quantity is highly variable because of external flux conditions. Thus this comparison is not particularly meaningful.

Even when Q_c is not neglible, account may be taken of its effects by using an effective area for surface radiative heat transfer to surroundings which is larger than the actual active region area. The appropriate effective "length"

of the active region for radiative heat transfer can be taken as

$$L' = L \frac{Q_R + Q'_R + 2Q_c}{Q_R + Q'_R}$$

As long as L meets the basic design criteria we will have an isothermal region surrounding the center of the active region.

B.2. TRANSIENT MODEL

A good approximation to the transient time constant can be obtained by considering the active region to be isothermal at temperature T_2 and with heat capacity C_s, then

$$(WtL') \ \rho_s C_s \ \frac{dT_2(t)}{dt} = (Q + Q' - Q_R - Q'_R)(WL') \qquad (10)$$

If $(Q + Q')$ is replaced by a step function source $Q_o U(t)$ the transient response can be evaluated; from

$$t\rho_s C_s \ \frac{dT_2(t)}{dt} = Q_o U(t) - \sigma \left[(1 + \varepsilon) \ T_2^{\ 4}(t) - (T_H^{\ 4} + \varepsilon T_o^{\ 4}) \right]$$

$$= Q_o U(t) - (1 + \varepsilon) \ \sigma T_x^{\ 3} \ (T_2(t) - T_a)$$

where

$$T_a^{\ 4} = \frac{T_H^{\ 4} + \varepsilon T_\sigma^{\ 4}}{1 + \varepsilon}$$

$$T_x^{\ 3} = (T_2^{\ 2} + T_a^{\ 2})(T_2 + T_a)$$

hence the characteristic time constant for transient temperature changes is

$$\tau = \frac{t\rho_s C_s}{(1+\varepsilon) \ \sigma T_x^{\ 3}} \quad \text{sec} \qquad (11)$$

where T_2 is taken to be $T_2(t)$ max in the expression for T_x.

III. <u>EXPERIMENTAL</u> <u>INVESTIGATIONS</u>

A.1. Introduction

The ultimate objective is to obtain a measure of an atomic beam flux. Using the basic thermal sensor configuration of figure 1, the surface recombination energy, related to the atomic beam flux, results in an elevated surface temperature over the active region of the sensor.

Two means for sensing temperature were investigated. The atomic recombination (active) surface is a thin metallic platinum film so it is natural to consider using the TCR of the metal as the sensing mechanism. In general as metallic film thicknesses are reduced, a point is reached where the electrical properties deviate significantly from that of the bulk material. Gold films become discontinuous when the thickness is reduced to less than about 100 $\overset{\text{o}}{\text{A}}$.. In this range the resistivity increases markedly, the TCR switches from positive to negative, and the magnitude reaches levels up to an order of magnitude greater than the bulk value. This increased TCR yields the high temperature sensitivity necessary to detect small temperature changes resulting from atomic recombination. If similar effects occur for platinum a highly sensitive atomic detector can be constructed.

The second method for temperature sensing uses a very small bead thermistor thermally bonded to the side of the substrate opposite to the active surface. Temperature changes due to recombination are transmitted through the film and are detected by changes in thermistor resistance. Since the TCR of bead thermistors is more than one order of magnitude greater than that of bulk platinum a very sensitive sensor again results.

Several advantages are gained by using the insulating mylar film/platinum film structure. The sensor heat transfer mechanism is radiation limited rather

than conduction limited as in the solid platinum wire detector. This results in an order of magnitude higher sensitivity because heat loss rate is reduced in like amount. Even thin films of mylar have very high physical strength and dimensional stability resulting in a mechanically rugged detector.

Mylar exhibits a high permeation rate for H_2. This should substantially reduce the saturation effects observed with solid platinum detectors by effectively removing the recombined H_2 adsorbed at the platinum surface which finally saturates the bulk metal. Finally with the bead thermistor geometry, heat supplied to the thermistor can be effectively used to maintain the active surface at an elevated equilibrium temperature further reducing the saturation effects.

As design parameters we use the conditions given in reference 2, namely, an atomic beam flux of 2×10^{13} atoms/cm^2·sec as our datum. Recombination energy $\epsilon = 3.52 \times 10^{-19}$ J/atom and surface efficiency, η, of 50%. The design minimum beam energy flux becomes $F = 35.2$ mW/M^2. All calculations refer to this datum level.

A.2. MATERIALS PROPERTIES

The active recombination surface for all investigations included in this report was a thin film of platinum. Film structure and deposition methods used will be discussed in a later section.

The substrate used for some of the thin film investigations was either barosilicate glass or aliminum ceramic. The substrate used in actual sensors was an 0.8 mil thick by 1.0 cm wide Dupont Mylar polyester film generally used as video recording tape. Thermal and electrical properties of bulk platinum and Mylar are given in Table I for an ambient temperature of 20°C.

TABLE 1

Property	Mylar	Bulk Platinum
Density - kg/M^3	1.377×10^3	21.45×10^3
Specific Heat - $J/Kg \cdot {}^oK$	1317.	134.2
Thermal Conductivity - $w/M \cdot {}^oK$	0.174	71.06
Bulk Resistivity - $\Omega.M$	- -	10.6×10^{-8}
TCR - $1/{}^oC$	- -	3.92×10^{-3}
Emissivity	~ 1.0	.037

B. DEVICE PARAMETERS

Based on the theory presented in section II we can evaluate the theoretical parameters expected using a Mylar/platinum film structure similar to that shown in figure 1. Since all temperatures encountered are close to room temperature of 20^oC we will assume all reference temperatures are close to 295^oK. Constants for the various materials are given in table 1.

On the substrate far from the active region $Q = Q' = 0$, Eq. (9) gives

$$T_1 - T_2 \cong .025 \left[1 - \frac{T_H^4}{T_o^4} \right] + 5.7 \times 10^{-5} (Q + \epsilon Q')$$

even if $T_H = 320^oK$, $T_1 - T_2 \cong .01 \ {}^oK$ so that the substrate is truly isothermal. In the active region the situation is even better since there we have $T_1 - T_2 \approx .0003 \ {}^oK$. From the above it is clear that we can neglect any temperature gradients from one side of the film to the other. In the active region then,

$$T_2{}^4 = 0.964 \left[T_H{}^4 + .037\, T_o{}^4 + \frac{1}{\sigma}\, (Q + Q') \right]$$

while for the region of the substrate away from the active region,

$$T_\infty{}^4 = 0.5\, (T_H{}^4 + T_o{}^4)$$

At the edge of the active region we have transverse temperature gradients with characteristic "diffussion length" given by Eq. (6a);

$$L_{D_a} = 7.5 \times 10^{-4}\ m$$

in the active region and

$$L_{D_s} = 5.4 \times 10^{-4}\ m$$

in the bare substrate region. The temperature at the edge of the active region is given by

$$T_o = 0.42\, T_2 + .58\, T_\infty\ {}^oK$$

At this point it should be noted that if the emissivity of mylar is taken as $\varepsilon_{\dot{m}} < 1$ the value for σ in the above equations is replaced by $\varepsilon_m \sigma$. This results in increased sensitivity of the device to changes in $Q + Q'$.

Checking the original approximation that Q_c can be neglected in the overall heat balance we get, for $L = 1.cm$

$$\frac{2Q_c}{Q_R + Q'_R}\ \frac{t}{L}\ < .15$$

a value consistent with the assumptions.

The thermal time constant may be obtained from equation (11) as

$$\tau = 5.9\ sec$$

From equation (5) we can estimate the temperature rise, ΔT, expected from the datum atomic flux previously given as 35.2 mW/M^2. Assuming for the moment $T_o = T_H = 295\ {}^oK$ we get,

$$\Delta T = 0.65\ F^oK$$

$$= 23\ m^oK$$

a value well within the realm of measurability. Assuming bulk resistivity
for the platinum film this corresponds to differential film resistance

$$\frac{\Delta R}{R} = 9 \times 10^{-5} \ \Omega/\Omega$$

C.1. THIN FILM PLATINUM RESISTORS

Since the initial concept was to provide a thin film platinum bolometer
with enhanced TCR, an investigation was initiated to obtain the TCR vs. film
thickness characteristic of Pt films. Film thickness, deposition rate, and
type of substrate were the experimental variables. Since a large mass of Pt
was not available the deposition rate was severely limited but still adequate.

The idea of using a Mylar film substrate evolved following difficulties
in obtaining sufficient temperature rise from ohmic heating of the film on glass
substrates. The desirability of this structure in providing a sensitive,
efficient detector became obvious after comparison with the original Pt wire
detector against which it should be about 2 orders of magnitude more sensitive.
Initially however, films were deposited on glass and ceramic substrates for
direct TCR determinations.

C.2. Pt FILM DEPOSITION SYSTEM

Throughout the experiments performed in this research, several items
remained the same. For the sake of convenience, some of these will be discussed
at the beginning, and only referred to later. The vacuum deposition system
used to deposit the thin films was a CVC vacuum system using a 4" oil diffusion
pump with a liquid nitrogen cooled baffle. In all cases the material was de-
posited with a Varian "e-gun" electron beam thin film deposition source, operated
at about 2kW power input.

Thickness of the films deposited was monitored during deposition with
a Sloan Digital Thickness Monitor. The measuring head was placed at an angle of
about 30 degrees from the vertical axis above the source. The deposition source
ejects material in approximately a cosine distribution. In all cases the substrate
to be deposited on was held about 25 cm from the source. The Sloan head was about

19 cm from the source. Applying the inverse square law to the source intensity we find the correction factor for the thickness read on the meter as $(19/25)^2$ $(\cos 30°)$, or about 0.5. When other factors are considered, such as sticking coefficient and possible departures from ideal source distributions, the thickness figures given are probably within a 20% accuracy bound. Since all of the thin films studied are less than 400 Å thick there were no other means available to measure thickness any more accurately during or after deposition, so the Sloan thickness monitor was used as the reference throughout.

Whenever a platinum thin film was made, the CVC system was pumped down to 10^{-5} torr or lower base pressure. The source of Pt for deposition was a wire coiled up and melted in the "e-gun", forming a bead about 1.5 mm in diameter.

C.3. Pt ON CERAMIC AND GLASS

The first films to be tested were either deposited on either 2" x 2" glass slide covers or unglazed ceramic substrates. Pt film resistors were made on each kind of substrate, with thicknesses of 1.5, 2.5 nm, and 7.5 nm. Two resistors were made on each substrate. Each resistor was 1.2 cm wide and 2.5 cm long. The deposition rate was about 0.2 nm/min.

To test the glass and ceramic resistors, leads were attached to the thin films with silver paste. First a 1 mil gold wire was attached to the film, and then to the substrate, at which point a larger, #20 copper wire was attached to the gold wire and the substrate. The substrates were then baked at 150°C for about 20 minutes to cure the silver paste.

The film resistors were placed in a separate sorption/ion pumped vacuum bell jar system constructed for this puspose. Resistance was measured using a Lambda variable voltage power supply, a PHE portable potentiometer, and a Leeds & Northrup millivolt potentiometer. The resistor under test was placed in series

with a precision 2002 ohm resistor and the power supply.

As film thickness was decreased the TCR (Temperature coefficient of resistivity) dropped from the bulk value to zero at approximately a film thickness of 5.0 nm. For thinner films the TCR became slightly negative, but never greater than the bulk value. These experiments proved rather difficult to perform because of the problems attendant with maintaining a large substrate at constant temperature and because of the small temperature rises attainable by direct ohmic heating of the surface film.

The remaining experiments were performed on a Mylar film substrate.

C.4. Pt FILMS ON MYLAR

An aluminum holder was machined to hold strips of mylar. It was made with two parallel vertical ridges which were 1 mm high and 3.0 cm apart. Two strips of mylar, 17 to 8 micrometers thick and 0.5 cm wide were stretched over the aluminum holder ridges and secured by clamping. A mask was placed over the mylar strips, and the Pt thin film deposited to make a resistor 1.0 cm long, and across the entire width of each strip. A pair of 1 mil gold wires was attached to each resistor with silver paste and the silver paste left to cure under vacuum. The whole apparatus was placed in the ion pump system. The resistance and power delivered to the test resistor was measured with varying levels of power input, causing a variable temperature rise due to ohmic heating.

The reference arm of the resistance measurement bridge was composed of 500 Ω low TCR precision resistors.

In order to obtain accurate surface temperature measurements a 10 KΩ 10. mil diameter glass bead precision thermistor (Fenwal Electronics) was attached to the Mylar on the side opposite the film. The thermistors used were purchased as matched pairs, one for each of the two Mylar strips. One

strip was used as the bridge reference resistor. Characteristics of the
thermistors were determined in an isothermal environment to be,

$$\ln R = - .04083T + 3.1663$$

where R is the resistance in $K\Omega$ and T the temperature in $^{\circ}C$. The above equation
is valid over a $40^{\circ}C$ temperature range.

Power input to the thermistor caused a error in the temperature measurement
due to substrate heating but since it remained constant at approximately 100 μW
throughout the experiments account may be taken of its effects by introducing
a Q' factor in the equation for surface temperature (eq.8). Accuracy of the
relative temperature measurements, was established at $\pm$ 5.0 $m^{\circ}K$.

Temperature of the structure was controlled independently by resistance
heating or water cooling the holder in the vacuum bell jar. According to the
radiative heat transfer theory previously described the substrate temperature
should and does accurately track the holder temperature. Ambient temperature
was monitored throughout the experiments.

Several resistor thicknesses were tested, one (at least two of each were
tested) approximately .5 nm thick at a resistance of 11.2 $G\Omega$ and another 7.5 nm
thick with 148 Ω resistance are representative. A 2.5 nm 10.5 $K\Omega$ resistor was
also tested using direct heating of the surface film.

The TCR of the 2.5 nm resistor was within measurement accuracy, zero. The
7.5 nm resistor showed a positive TCR of .0002 Ω/Ω . $^{\circ}C$ or about one order of
magnitude below the bulk value of .003 $\Omega/\Omega.^{\circ}C$. As expected the .5 nm film re-
sistor showed a negative TCR of 0.002 $\Omega/\Omega.^{\circ}C$, a value close to but less than
the bulk.

Although the TCR does eventaully become negative it never attains values
greater than that of the bulk material. In addition when larger TCR values are
finally reached, the surface coverage of platinum is far too small for it to act

as an effective atomic recombination center.

Apparently Pt because of its low surface mobility at attainable substrate temperatures does not agglomerate during deposition. Thus the large TCR ($\simeq$ 1.0) achievable with ultrathin gold films is not possible with Pt. The large film resistivity observed in the present experiments, although consistent with values for agglomerated films, is due to primarily to large unannealed stresses in the film induced during deposition. Presence of these (tensile) stresses is indicated by a slight curling toward the Pt surface of the edges of the Mylar substrate. Previous work with Pt films[3] indicates high substrate temperatures ($\sim$400°-600°C) during deposition could indeed provide agglomeration. We must therefore conclude that the ultra-thin film Pt resistor type sensor is not a viable configuration. It still remains possible to place a thick Pt film on one side and ultra-thin Au on the other side of the substrate as the temperature sensor element.

C.5. THERMISTOR SENSOR

In the course of testing the Pt films it was determined that a thermistor/thick Pt film on Mylar combination yielded excellent sensitivity to thermal flux at the platinum surface.

Four of these devices were constructed and tested. Applying the theory given previously to these devices a predicted sensitivity to atomic flux at the surface should yield 22.m°C temperature rise for the datum atomic flux density of 2×10^{13} atoms/sec/cm^2. This should result in a measurement sensitivity in the thermistor bridge circuit of .25 mV for the above atomic flux density. This value is a factor of 100 better than the Pt wire detector previously mentioned. In addition we gain the structural strength of the Mylar substrate structure.

In order to test the devices without actually inserting them in the discharge bulb system, a 400 μW HeNe laser beam was defocused and used to simulate

the atomic flux. The laser output was calibrated and surface power absorption was determined. Based on these measurements the sensitivity was determined to be a factor of 10 below that predicted. In any case this corresponds to a over-all system sensitivity of 25 μV/2 x 10^{13} atoms/cm^2·sec, much better than pre-viously achieved. In addition the thermal mass reduces noise levels and drift to easily manageable levels. Curves of thermal and thermistor bridge response to surface energy flux are shown as figures 3 and 4 for two different sensors.

The thermal response time was determined by pulsing the laser heat source at the recombination surface. The time constant was determined to be 2.4 sec a factor of 2.0 less than the predicted value. This result is consistent with the added heat loss through the thermistor lead wires.

In order to test the theory further and confirm the general validity, the laser beam was collimated (beam diameter ~ 1.0 mm) and scanned across the surface film. A value for L_D was determined in this way by measuring thermistor temperature rise versus distance of the laser spot from the position of the thermistor on the reverse side of the film. L_D is the traverse distance for which the temperature rise of the thermistor falls to 1/e of the coincident value. The observed result was L_D = 1.5 mm, a factor of two greater than predicted again because of the lead wires.

D. RESULTS AND CONCLUSIONS

The experimental errors are explained by the fact that the thermistor sensor acts as a small area heat source on the mylar substrate. Because of this the effective surface heat flux density Q' is much larger than that of a dis-tributed source at the same power level. Assuming the entire heat input to the thermistor is distributed over a 1 mm^2 area the sensitivity factor of 10 is accounted for. Accounting for the conduction loss of the 1 mil Pt leads to the thermistor combined with the additional thermal mass introduced by the 1 mil
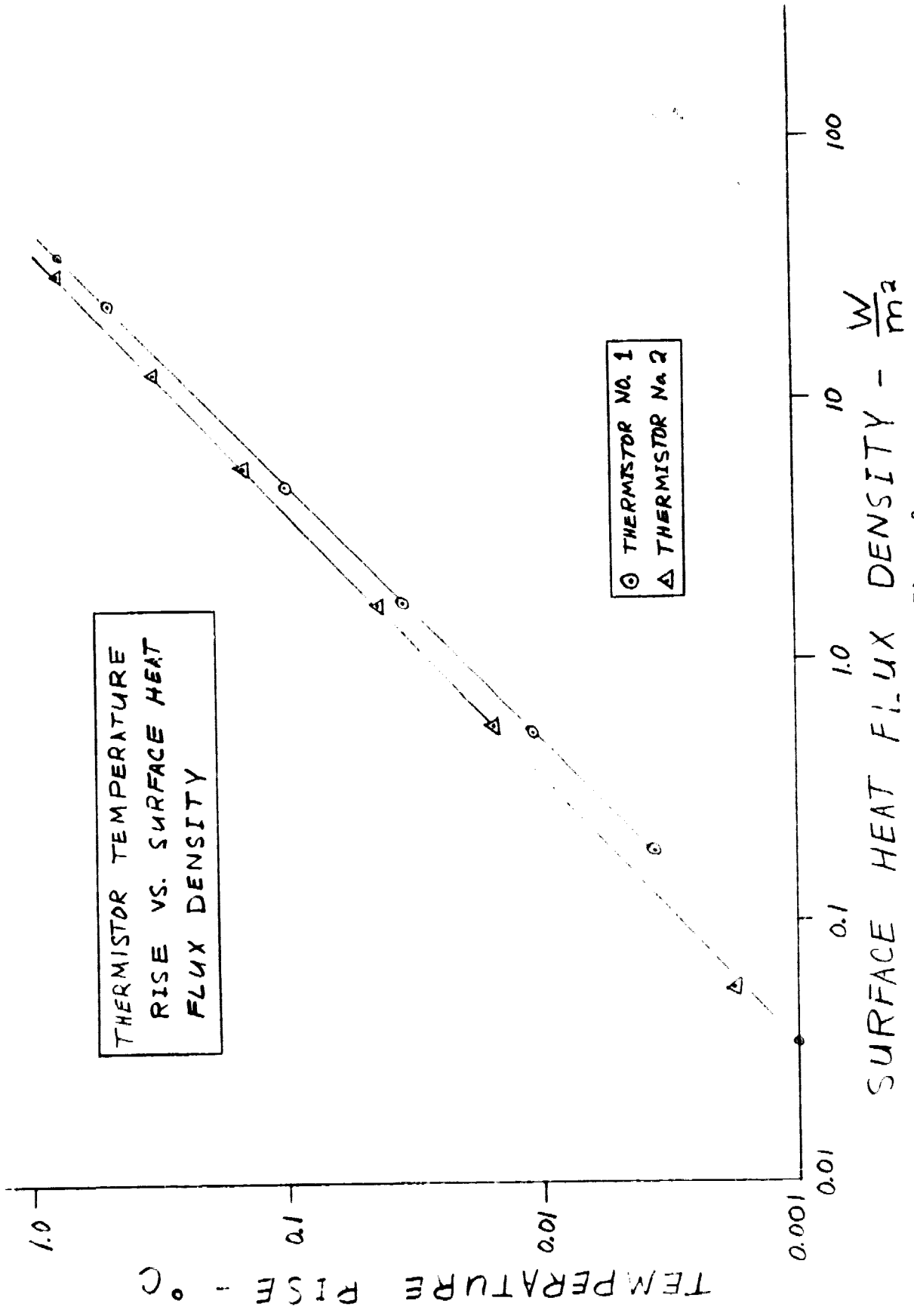
THERMISTOR TEMPERATURE RISE VS. SURFACE HEAT FLUX DENSITY

⊙ THERMISTOR NO. 1
△ THERMISTOR No. 2

SURFACE HEAT FLUX DENSITY – $\frac{W}{m^2}$

Figure 3

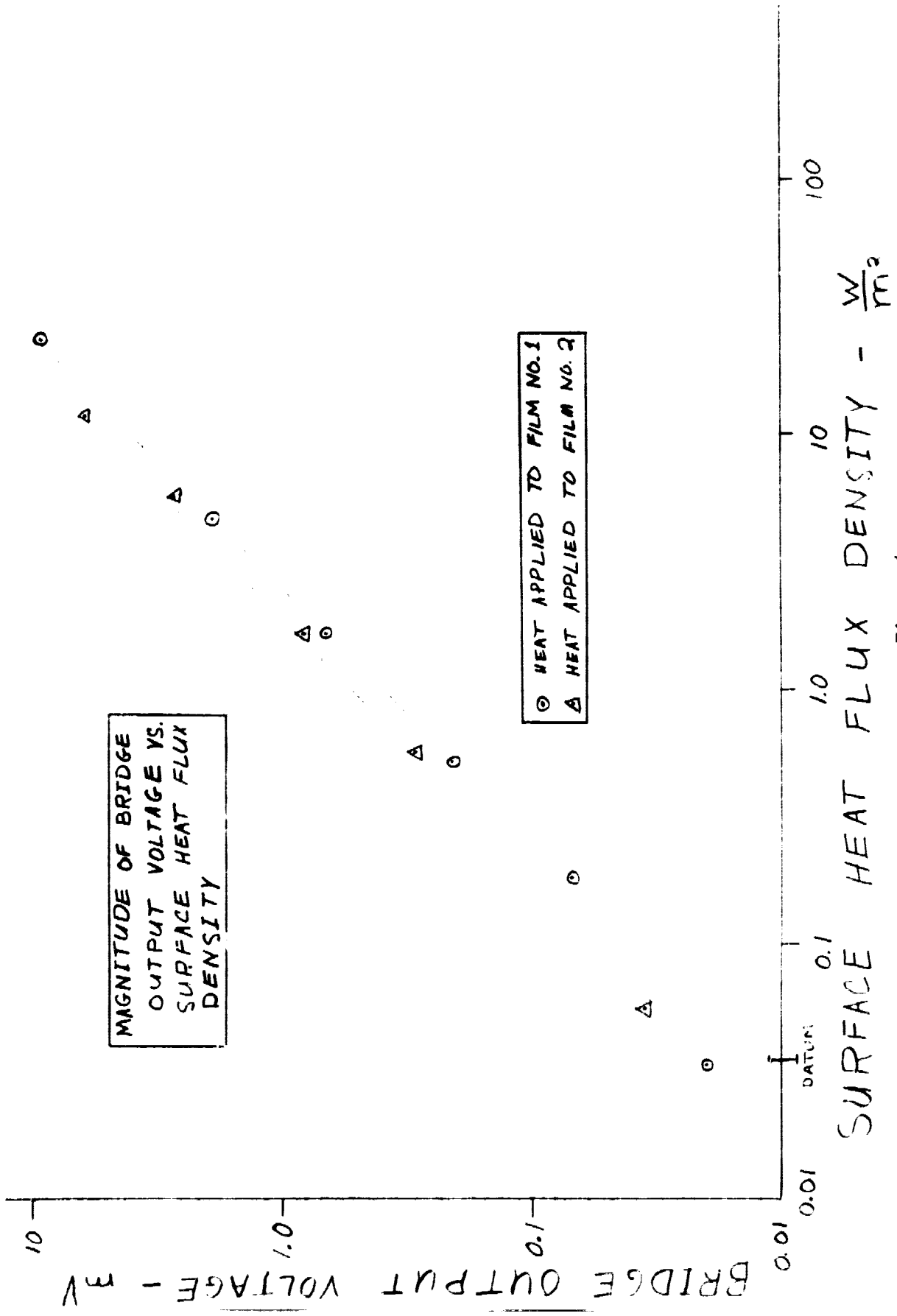TEMPERATURE RISE – °C

23

Figure 4

bead brings the thermal time constant to within a factor of 1.5 of the predicted value. The basic theory of radiation limited detection is reasonably well confirmed by all experiments.

Finally the calibration procedure using a laser as a precision heat flux source allows absolute calibration of the detectors to within an accuracy of ± 10%. With a distributed thermistor on the back of the Mylar and with reduced power input to the sensor we could reasonably expect to gain yet another order of magnitude in detection sensitivity.

Further development has yielded a new sensor using a platinum foil with attached bead thermistor supported and thermally insulated by bonding to the Mylar film to the edges. Because the Pt foil becomes an isothermal surface the detection sensitivity is even higher than that of the all Mylar structure. This device should yield 80 μV bridge output for our datum atomic flux density.

A detector unit is now being constructed that will be supplied to NASA if so desired.

APPENDIX

In the process of assembling and testing the vacuum system for evaluating RF discharge dissociators it was determined that the conventional palladium leak hydrogen sources were neither stable nor accurately controllable enough to be used in atomic hydrogen flux measurements.

To obtain precise hydrogen gas flow control an electrolytic cell hydrogen generator was obtained from Lab Data Control Corp. in St. Petersburg, Florida.

With this device the hydrogen permeation rate through a Pd membrane is controlled by a DC current flow through the electrolytic cell. Of primary importance to our system operation are the generator characteristics as follows:

(1) Gas purity as evidenced by attainable vacuum system base pressure under zero cell current conditions.

(2) Electrical power input

(3) Proportionality between cell electrical current and hydrogen generation (flow) rate at low back pressures (~100 mtorr in this case).

(4) Cell flow time constant with respect to step changes in cell current.

(5) Stability relative to changes in ambient conditions.

As installed in the vacuum system, connections are made via copper tubing with a Swagelok compression fitting at the cell and soft solder at the vacuum system entry point.

After one month of pumping with no bakeout, the vacuum system base pressure achieved is 2×10^{-9} torr as obtained from the ion pump current with manufacturer supplied calibration curves. This would indicate a gas purity under normal operating conditions of less than 0.1 ppb impurity concentration.

Electrical power requirements for the cell are 1.2 - 1.3 VDC with cell
current varying from zero to 10 mA depending on gas flow rate requirements.
Using the usual 91 orifice effuser approximately 2 mA should be sufficient to
maintain a discharge bulb pressure of 100 mtorr. It can be seen that the power
requirement is several orders of magnitude below that for a thermal palladium
leak.

The operating characteristic of the cell under our conditions could not
be obtained from the manufacturer so a series of tests were run with the ion
pump as the measurement device. The characteristic herein referred to is
hydrogen flux, Q-torr·ℓ/sec, versus cell input current I-mA. In principle a
one-to-one linear relationship should exist. Ion pump pressure, p, is obtained
from the pump current vs. pressure conversion chart. This value is corrected
for hydrogen by the usual multiplicative factor of 2.7. Throughout, Q is
obtained by multiplying the measured result by the manufacturer supplied values
of pumping speed versus pressure. The latter represents only a small correction
simce the pump is essentially constant speed in the pressure range of interest
here. Cell current is obtained with a digital milliammeter.

Figure 5 shows the results. The offset is due to meter error in the ion
pump controller. It is clear that within the measurement accuracy ($\pm$ .02% and
$\pm$ 0.1% for Q and I respectively) the cell characteristic is quite linear with
slope of 0.086 $\frac{Torr \cdot \ell}{sec \cdot A}$. Mathiessen Corporation a supplier of the unit quotes
the range of values for mean slope as 5.0 to 7.7 SCCm/A for units operated at
elevated temperature and back pressure of up to 10 atm. Our value (converting
Q to SCCm units) compares very favorably at 6.8 SCCm/A. Since the hydrogen
generation characteristic is linear a simple feedback control system can provide
very precise control of flow rate. This is especially true since no variation

of H_2 flow rate was observable over an ambient temperature range of $68 \pm 5^\circ F$.

Water consumption over a 3 month period was negligible at a cell current of 2.0 mA. Evaporation contributed the small amount of reservoir water loss observed.

Response of the cell to step changes in cell current depends strongly on the initial and final current levels. In all cases the response time is measured in minutes. The effect is caused by saturation of the palladium during steady state operation and the requirement for reaching a new volume saturation condition coupled with the naturally low permeation rate. The response time appears to be linearly dependent upon flow rate (cell current). With a step change in cell current from 5.0 mA to 3.0 mA the equivalent exponential time constant is 45 ± 5 minutes.

The very long time constant offers distinct advantages over the more responsive palladium leak purifier in that any rapid fluctuations in cell current and ambient temperature have negligible effect upon the flow rate. One difficulty arising from the time factor is that the flow cannot rapidly be "shut-off" without use of an external valve and any flow control system would necessarily be sluggish unless large loop gains are incorporated.

Feedback control of flow using a vacuum gauge as the sensing element is very effective in any case due to the sensitivity of flow rate to changes in current ie., the response of a typical bulb-effuser system operating at p = 100 mtorr with effuser conductance of 2ml/sec yields a current sensitivity of 43 $\frac{mtorr}{mA}$.

It is strongly recommended that the electrolytic hydrogen generator be seriously considered for use in all future atomic clock systems. Not only is this device more convenient and stable from a systems viewpoint but in addition has a virtually unlimited lifetime according to the manufacturer.
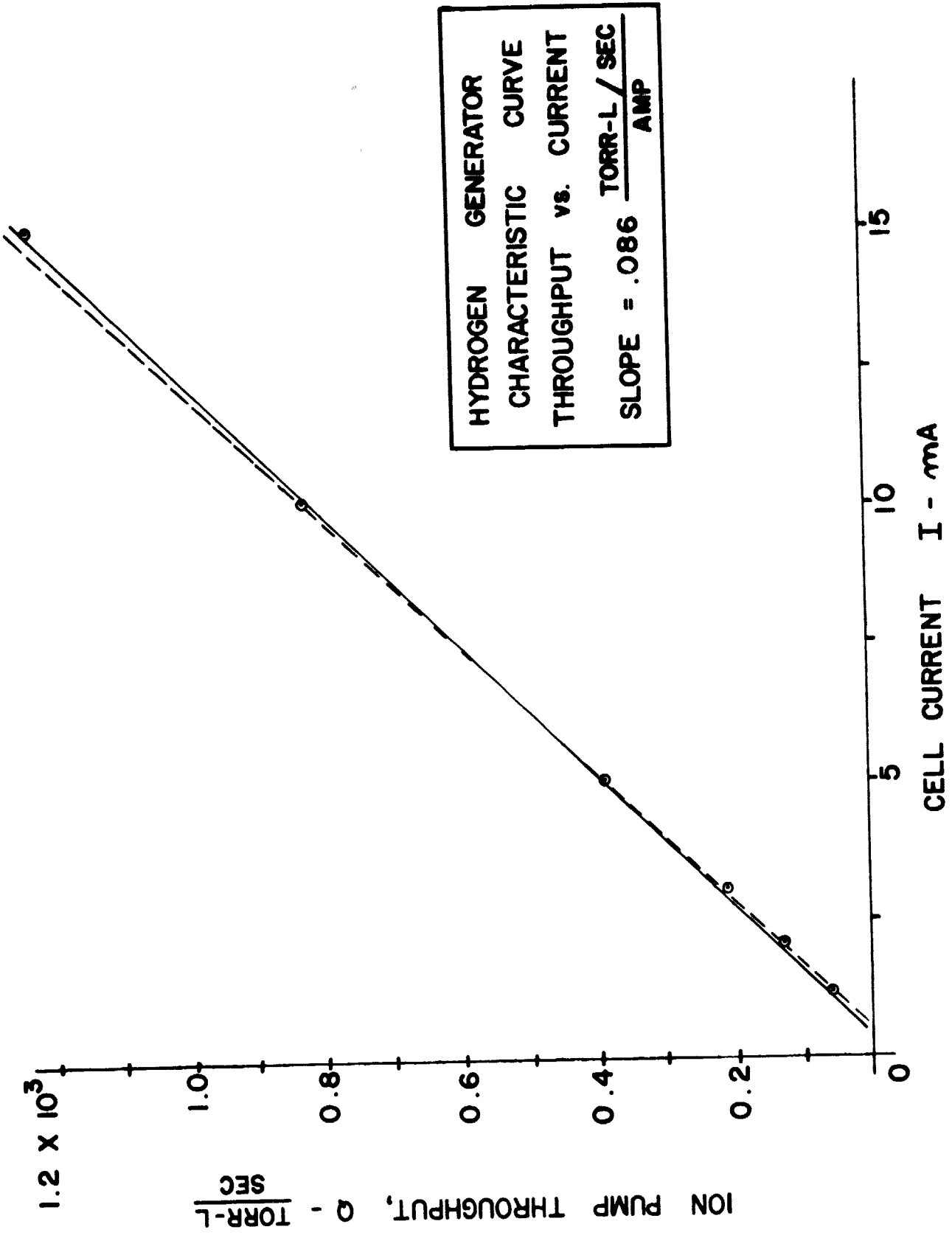
HYDROGEN GENERATOR
CHARACTERISTIC CURVE
THROUGHPUT vs. CURRENT

$$SLOPE = .086 \frac{TORR\text{-}L / SEC}{AMP}$$

CELL CURRENT I - mA

ION PUMP THROUGHPUT, Q - $\frac{TORR\text{-}L}{SEC}$

Figure 5

BIBLIOGRAPHY

1. Peters, Harry E., <u>Topics in Atomic Hydrogen Standard Research and Applications</u>, Goddard Space Flight Center, Greenbelt, Md., October 1971. [x-524-71-408 preprint]

2. Brenner, Douglas, "Regulation of Atomic Hydrogen Flow with a Platinum Wire Detector," <u>The Review of Scientific Instruments</u>, Vol. 40, No. 9, 1234-1235, (September 1969).

3. Maisel, Leon I. and Glang, Reinhard (eds.), <u>Handbook of Thin Film Technology</u>, McGraw-Hill Book Company, New York, 1970.